# Short-range and long-range magnetic ordering in $\alpha$-$CuV_2O_6$

A. N. Vasil'ev and L. A. Ponomarenko
*Department of Physics, Moscow State University, Moscow 119899, Russia*

A. I. Smirnov
*P.L. Kapitza Institute for Physical Problems of RAS, Moscow 117334, Russia*

E. V. Antipov and Yu. A. Velikodny
*Department of Chemistry, Moscow State University, Moscow 119899, Russia*

M. Isobe and Y. Ueda
*Materials Design and Characterization Laboratory, Institute for Solid State Physics, University of Tokyo, Roppongi 7-22-1, Tokyo 106, Japan*

(Received 12 October 1998)

Magnetic properties of the triclinic copper vanadate $\alpha$-$CuV_2O_6$ with linear chains of edge-sharing $CuO_6$ octahedra were studied by magnetic susceptibility and electron-spin-resonance measurements. The broad maximum of a magnetic susceptibility at $T_M = 44$ K corresponding to the intrachain exchange interaction $J = 34$ K indicates one-dimensional short-range magnetic ordering within the chains. Three-dimensional long-range antiferromagnetic ordering takes place at $T_N = 24$ K, suggesting a rather large value for the interchain exchange interaction $J_\perp \sim 16.5$ K. The energy gap found in the antiferromagnetic resonance spectrum 76 GHz agrees with the spin-flop magnetic-field value of about 2.7 T. [S0163-1829(99)05825-7]

The copper- and vanadium-based complex oxides are frequently found among those inorganic compounds which exhibit a low-dimensional magnetic behavior at lowering temperature. Besides other spin-chain and spin-ladder compounds this behavior was observed recently in $CuM_2O_6$ ($M$ = Sb, Nb) compounds. While being of the same chemical formula these compounds possess different crystal structures and therefore different albeit quasi-one-dimensional arrangements of magnetic ions.

In the monoclinic copper antimonate $CuSb_2O_6$ the main building blocks are constituted by edge and corner sharing $CuO_6$ and $SbO_6$ octahedra. The magnetic $Cu^{2+}$ ions forming square lattices in the $a$-$b$ plane are separated from each other by two sheets of nonmagnetic $Sb^{5+}$ ions along the $c$ axis. The dominant antiferromagnetic interaction occurs through a linear Cu-O-O-Cu linkage which connects one set of two next-nearest-neighbor $Cu^{2+}$ ions. The interaction with other two next-nearest-neighbor $Cu^{2+}$ ions is frustrated, providing a dominance of quasi-one-dimensional in-plane interaction. The $CuSb_2O_6$ exhibits a broad maximum of magnetic susceptibility at $T_M = 60$ K and the transition to antiferromagnetic state at $T_N = 8.5$ K.[1]

The copper niobate was investigated in both monoclinic $\alpha$-$CuNb_2O_6$ and orthorhombic $\beta$-$CuNb_2O_6$ polymorphs. Both structures contain zigzag chains of edge-sharing $CuO_6$ octahedra, separated by chains of edge-sharing $NbO_6$ octahedra forming washboardlike planes by the linkage of corner oxygens. The ground state of the $\alpha$-$CuNb_2O_6$ is separated by a spin gap from the excited states due to the alternating exchange coupling between the $Cu^{2+}$ spins within the quasi-one-dimensional chains.[2] The $\beta$-$CuNb_2O_6$ exhibits a broad maximum of magnetic susceptibility at $T_M = 20$ K followed by antiferromagnetic transition at $T_N = 7.5$ K.[3]

The copper vanadate $CuV_2O_6$ has attracted attention recently as another $CuM_2O_6$ compound containing linear chains of $Cu^{2+}$ ions in $\alpha$-phase. Its triclinic $C1$ polymorph's lattice parameters are $a = 9.168$ Å, $b = 3.543$ Å, $c = 6.478$ Å, $\alpha = 92.25°$, $\beta = 110.34°$, and $\gamma = 91.88°$.[4] As shown in Fig. 1, the structure of this compound can be derived from a hexagonally pseudo-close-packed arrangement of $O^{2-}$ ions with both $Cu^{2+}$ and $V^{5+}$ ions octahedrally coordinated and (101) as the stacking direction. Each $CuO_6$ group shares two edges with $CuO_6$ groups displaced by a $b$-axis translation; within the chains the Cu-Cu distance is 3.58 Å and the Cu-O-Cu bond angle is 97.9°. The $CuO_6$ octahedra chains are separated from each other by double chains of $VO_6$ octahedra; the distance between Cu ions in adjacent

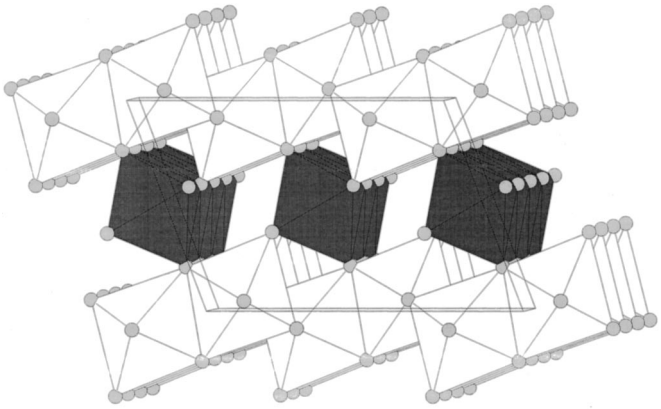

FIG. 1. The polyhedra representation of the crystal structure of $\alpha$-$CuV_2O_6$. The $Cu^{2+}$ ions are situated within the dark-shaded octahedra at the corners of the unit cell and at the centers of the $a$-$b$ planes.

 

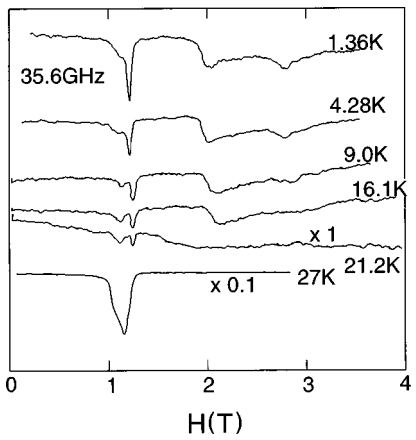


FIG. 2. The temperature evolution of the ESR spectrum in $\alpha$-$CuV_2O_6$ at 35.6 GHz.

chains is 4.927 Å. The NMR report on $CuV_2O_6$ is available indicating antiferromagnetic long-range ordering at 23 K,[5] and recent neutron-scattering experiments evidenced non-negligible interchain interactions in this compound.[6]

We performed electron-spin-resonance (ESR) and magnetic-susceptibility studies on powder samples of $\alpha$-$CuV_2O_6$ synthesized by a conventional solid-state reaction of a stoichiometric mixture of CuO and $V_2O_5$ in air at 600 °C. The formation of copper vanadate at this temperature was fast and required only a few days, but the sample so prepared invariably contained some amount of ferromagnetic $Cu_2V_2O_7$ phase. Multiple intermittent regrinding and sintering for two weeks resulted in a formation of a yellow-colored, almost single-phased, sample verified by x-ray powder diffraction.

The ESR spectra were taken using the microwave spectrometer of the transmission type. The rectangular resonator possessed several Te($01n$) modes in the range 20–75 GHz, which is the frequency range of the present study. The powder sample was inserted into the resonator in a foam container 2.0 mm in diameter and 1.5 mm in height. At high temperatures the ESR spectrum consisted of a single line of non-Lorenzian form with the average $g$ factor of 2.03. The temperature evolution of this line is shown in Fig. 2 for the frequency 35.6 GHz. The intensity of the single ESR line drops rapidly at $T_N = 24$ K. The weak line at $g \sim 2$ remains at lower temperatures and the broad magnetic-field band of weak absorption arises at temperatures below $T_N$. At low temperatures, at least two sharp singularities are seen in the absorption band. These singularities are marked by the triangles in Fig. 3, which shows the low-temperature spectra taken at various frequencies. The ESR lines corresponding to free-electron spins are marked by arrows. The rapid decrease of a paramagnetic signal at $T_N = 24$ K and transformation of the ESR spectra at low temperatures indicate transition of the sample into the long-range antiferromagnetic state.

In the absence of a magnetic field the maxima of microwave absorption at fixed frequency were detected at two different temperatures. The records of the transmitted microwave power vs temperature taken at various frequencies are shown in Fig. 4. The peaks of absorption are marked by arrows. The inset represents the temperature dependence of the ''zero-field'' resonant frequencies. The appearance of

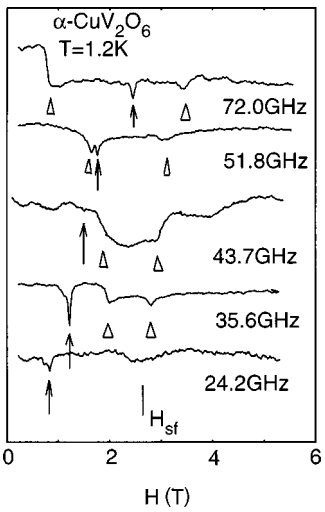


FIG. 3. The ESR spectra in $\alpha$-$CuV_2O_6$ taken at various frequencies at 1.2 K.

two energy gaps which increase at lowering temperature is what is to be expected for the spectrum of the antiferromagnetic resonance (AFMR) spectrum of a two-axis antiferromagnet.

The AFMR spectrum for this type of magnetic anisotropy[7] is shown in Fig. 5. The dashed lines represent two AFMR frequencies for the magnetic field parallel to the easy, the second easy, and the hard axes of sublattice magnetization. The values of the two AFMR gaps are taken here as 76 and 185 GHz. These two parameters fully determine the dependencies shown by the dashed lines in Fig. 5. The dashed lines in the inset of Fig. 4 correspond to the temperature dependencies of the AFMR gaps calculated in the molecular-field approximation with the gaps of 76 and 185 GHz at $T = 0$. The area marked by tilted lines corresponds to the resonance absorption in powder. The singularities in the absorption bands marked in Fig. 3 are represented here by

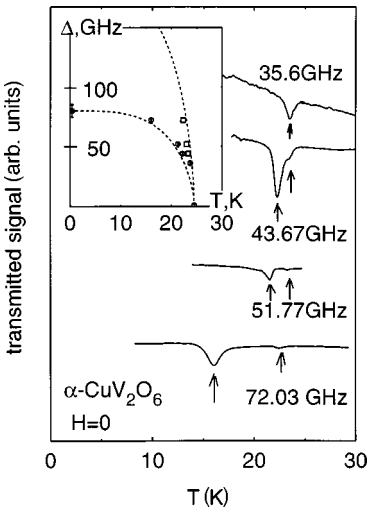


FIG. 4. The AFMR in $\alpha$-$CuV_2O_6$ at zero magnetic field (at the gap frequencies). The inset shows the temperature dependencies of the AFMR gaps. The lower gap value at 1.2 K is obtained from the spin-flop magnetic field of 2.7 T as shown in Fig. 5, and the zero-gap point is placed at $T_N$. The dotted curves in the inset represent the molecular field theory calculation.

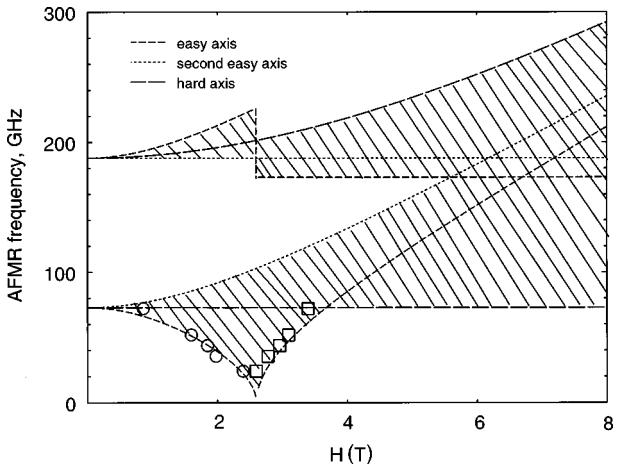


FIG. 5. The AFMR spectrum and the absorption bands in $\alpha$-$CuV_2O_6$. The AFMR gaps are taken equal to 76 and 185 GHz, and the spin-flop magnetic field is taken as 2.7 T.

circles and squares. Evidently, the boundaries of the absorption bands fit well to the spectrum suggested. The value of the lower AFMR gap at $T=0$ estimated based on this spectrum is 76 GHz, which corresponds to the spin-flop transition magnetic field 2.7 T.

The magnetic susceptibility $\chi$ of a pellet of $\alpha$-$CuV_2O_6$ was measured by a Quantum Design superconducting quantum interference device (SQUID) magnetometer. As shown in Fig. 6, the temperature dependence of $\chi$ taken at $H=1$ T exhibits a broad maximum at $T_M=44$ K and a subsequent decrease at lowering temperature. A small Curie-Weiss term, $\chi=C/(T\cdot\Theta)$, can be separated at low temperatures with $C=0.3\%$ and $\Theta=1\pm0.4$ K and is assumed to be due to the traces of other phases. No well defined anomaly indicating the transition into a long-range magnetically ordered state was observed in the smooth $\chi(T)$ dependence. The field dependencies of magnetization, however, qualitatively change at lowering temperature, as shown in Fig. 7. The change of

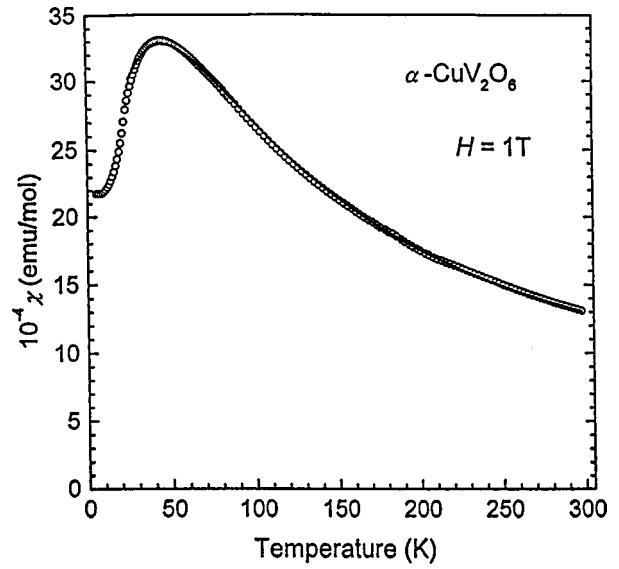


FIG. 6. The temperature dependence of the magnetic susceptibility of $\alpha$-$CuV_2O_6$ at $H=1$ T. The solid line represents a Bonner-Fisher fit with $T_M=44$ K, $g=2.03$, and $\chi_0=1.5\times10^{-4}$ emu/mol.

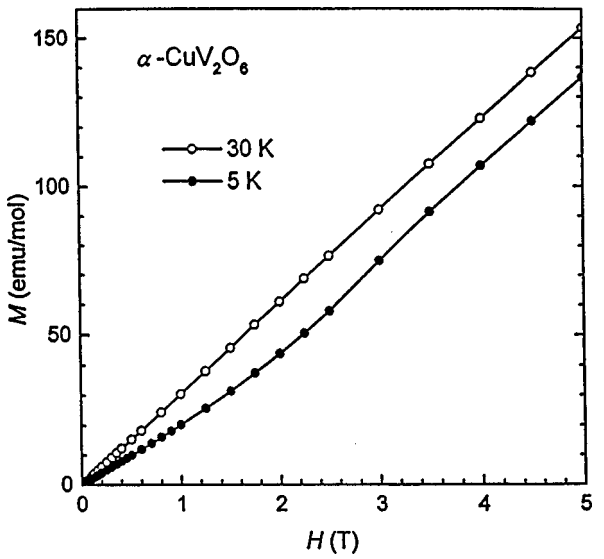


FIG. 7. The field dependencies of the $\alpha$-$CuV_2O_6$ magnetization at 5 and 30 K.

slope on $M(H)$ curves at low temperature indicates the spin-flop transition in three-dimensional antiferromagnets.

The broad maximum on the temperature dependence of a magnetic susceptibility is a landmark of low-dimensional short-range magnetic ordering. The calculations of the magnetic susceptibility for a spin $S=\frac{1}{2}$ Heisenberg linear chain are due to Bonner and Fisher.[8] They obtained $\chi$ at $T_M$ as

$$\chi_M=0.0735\,Ng^2{\mu_B}^2/J, \tag{1}$$

where $N$ is the Avogadro number, $\mu_B$ is the Bohr magneton, $k_B$ is the Boltzmann constant, and $J$ is the intrachain exchange integral. The fitting of experimental data by the Bonner-Fisher curve with the temperature-independent term $\chi_0=1.5\times10^{-4}$ emu/mol, $g=2.03$, and $T_M=44$ K, gives $J=34$ K.

The three-dimensional antiferromagnetic phase transition results from the coupling between the chains. The interchain exchange interaction $J_\perp$ in quasi-one-dimensional structures can be estimated using the expression[9]

$$J_\perp=\frac{T_N}{1.28\sqrt{\ln(5.8J/T_N}}. \tag{2}$$

This results in the interchain exchange integral $J_\perp\sim16.5$ K.

It is instructive to compare short-range $T_M$ and long-range $T_N$ magnetic ordering temperatures in order to elucidate the role of different magnetic ion arrangements in various $CuM_2O_6$ ($M=$ V, Nb, Sb) compounds. As can be seen in Table I, the ratios of $T_N$ to $T_M$ being approximately one half

TABLE I. Relevant magnetic data for $CuM_2O_6$ ($M=$ V, Nb, Sb) compounds.

| Compound | $T_M$ (K) | $T_N$ (K) | $J$ (K) | Reference |
|---|---|---|---|---|
| $CuSb_2O_6$ | 60 | 8.5 | 43 | 1 |
| $\beta$-$CuNb_2O_6$ | 20 | 7.5 | 34 | 2, 3 |
| $\alpha$-$CuV_2O_6$ | 44 | 24 | 34 | Present work |

in both linear ($\alpha$-$CuV_2O_6$) and zigzag ($\beta$-$CuNb_2O_6$) chain compounds differ significantly from that in a quasilinear arrangement of the magnetic ions in the nearly square planar lattice of $CuSb_2O_6$. In the latter case, the reduction of the long-range magnetic ordering temperature could be due to the strong frustration of the interchain interaction in the planes.

In conclusion, we showed that $\alpha$-$CuV_2O_6$ exhibits a transition from the short-range quasi-one-dimensional ordering at elevated temperatures into the long-range three-dimensional antiferromagnetic ordering at $T_N = 24$ K. The intrachain and interchain exchange integrals are estimated to be $J = 34$ K and $J_\perp \sim 16.5$ K, correspondingly. At low temperature $\alpha$-$CuV_2O_6$ possesses the spin-wave spectrum with two gaps of $76 \pm 3$ and $185 \pm 15$ GHz and exhibits a spin-flop transition at about 2.7 T.

The present work was supported by the Russian Foundation for Basic Research under Grant Nos. 96-02-19474 and 98-02-16572. One of the authors (A.N.V.) acknowledges the kind hospitality of the members of Materials Design and Characterization Laboratory, ISSP.

[1] A. Nakua, H. Yun, J. N. Reimers, J. E. Greedan, and C. V. Stager, J. Solid State Chem. **91**, 105 (1991).
[2] K. Kodama, T. Fukamachi, H. Harashima, M. Kanada, Y. Kobayashi, M. Kasai, H. Sasaki, M. Sato, and K. Kakurai, J. Phys. Soc. Jpn. **67**, 57 (1998).
[3] S. Mitsuda, J. Miyamoto, S. Kobayashi, K. Miyatani, and T. Tanaka, J. Phys. Soc. Jpn. **67**, 1060 (1998).
[4] C. Calvo and D. Manolescu, Acta Crystallogr., Sect. B: Struct. Crystallogr. Cryst. Chem. **29**, 1743 (1973).
[5] K. Ishiguchi, J. Kikuchi, K. Motoya, N. Eguchi, K. Inari, and J. Akimitsu (unpublished).
[6] J. Kikuchi, K. Motoya, K. Inari, N. Eguchi, and J. Akimitsu (unpublished).
[7] T. Nagamiya, K. Yosida, and R. Kubo, Adv. Phys. **4**, 1 (1955).
[8] J. C. Bonner and M. E. Fisher, Phys. Rev. A **135**, 640 (1964).
[9] H. J. Schulz, Phys. Rev. Lett. **77**, 2790 (1996).